

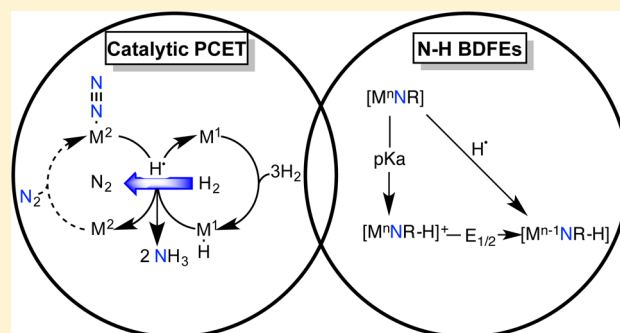
Catalytic Proton Coupled Electron Transfer from Metal Hydrides to Titanocene Amides, Hydrazides and Imides: Determination of Thermodynamic Parameters Relevant to Nitrogen Fixation

Iraklis Pappas and Paul J. Chirik*

Department of Chemistry, Princeton University, Princeton, New Jersey 08544, United States

S Supporting Information

ABSTRACT: The hydrogenolysis of titanium–nitrogen bonds in a series of bis(cyclopentadienyl) titanium amides, hydrazides and imides by proton coupled electron transfer (PCET) is described. Twelve different N–H bond dissociation free energies (BDFEs) among the various nitrogen-containing ligands were measured or calculated, and effects of metal oxidation state and N-ligand substituent were determined. Two metal hydride complexes, $(\eta^5\text{-C}_5\text{Me}_5)(\text{py-Ph})\text{Rh-H}$ (py-Ph = 2-pyridylphenyl, $[\text{Rh}]\text{-H}$) and $(\eta^5\text{-C}_5\text{R}_5)(\text{CO})_3\text{Cr-H}$ ($[\text{Cr}]^{\text{R}}\text{-H}$, R = H, Me) were evaluated for formal H atom transfer reactivity and were selected due to their relatively weak M–H bond strengths yet ability to activate and cleave molecular hydrogen. Despite comparable M–H BDFEs, disparate reactivity between the two compounds was observed and was traced to the vastly different acidities of the M–H bonds and overall redox potentials of the molecules. With $[\text{Rh}]\text{-H}$, catalytic syntheses of ammonia, silylamine and N,N -dimethylhydrazine have been accomplished from the corresponding titanium(IV) complex using H_2 as the stoichiometric H atom source. The data presented in this study provides the thermochemical foundation for the synthesis of NH_3 by proton coupled electron transfer at a well-defined transition metal center.



INTRODUCTION

The synthesis of NH_3 from its elements, N_2 and H_2 , is a long-standing challenge of both fundamental and practical importance.¹ In 2015, global ammonia production was in excess of 146 million metric tons, approximately 80% of which was used as crop fertilizer.² Nitrogen fixation schemes that are compatible with renewable rather than steam-reformed and hence fossil-fuel-derived hydrogen³ as well as operate in batch conditions are key components of carbon neutral ammonia synthesis.

Molecular catalysts for the fixation of N_2 to NH_3 are attractive not only for batch ammonia synthesis but also for developing the fundamental coordination chemistry and ligand design concepts for N–H bond formation. The “Chatt cycle”, a hypothetical and pedagogical scheme for the stepwise conversion of coordinated dinitrogen to ammonia,⁴ has provided the blueprint for subsequent catalyst development. Early demonstrations by Chatt and Hidai with phosphine-ligand molybdenum(0) dinitrogen compounds treated with mineral acids were valuable in illustrating the potential of this concept but were limited to stoichiometric NH_3 generation because the metal served as the sole source of the reducing equivalents.⁵ Pickett later reported use of a mercury pool cathode as an external reductant and demonstrated ammonia synthesis by electrolysis (-2.6 V vs Fc/Fc^+) of a bis-(phosphine) tungsten compound in the presence of strong acid.⁶ Shilov also reported catalytic ammonia and hydrazine

synthesis at 150 atm of N_2 with up to 10 000 turnovers, using $\text{Ti}(\text{OH})_3$, phosphine/phospholipid mixtures in the presence of catalytic $\text{Mo}(\text{III})$.⁷

More recently, Schrock and Nishibayashi demonstrated that molybdenum coordination compounds, upon treatment with sources of protons and electrons, are active catalysts for the reduction of N_2 to ammonia.⁸ In the latter examples, ligand modifications have produced turnover numbers in excess of 50. Peters and co-workers have applied a similar approach, using $[\text{H}(\text{OEt}_2)_2][\text{BAr}^{\text{F}}_4]$ ($\text{Ar}^{\text{F}} = \text{C}_6\text{H}_3\text{-}3,5\text{-}(\text{CF}_3)_2$) and KC_8 for iron⁹ and cobalt¹⁰ catalyzed N_2 fixation and most recently Nishibayashi has used the same proton and electron sources with pincer iron compounds for up to four turnovers of ammonia.¹¹

It is instructive to evaluate the energetic efficiency of these reactions compared to the Haber–Bosch reaction, nitrogenase enzymes or other hypothetical N_2 fixation schemes using H_2 as the source of protons and electrons. The Bordwell equation allows computation of the effective bond dissociation free energy of the reagent pair, e.g., the acid and electron source, as a function of pK_a and redox potential (eq 1):

$$\text{BDFE} = 1.37(\text{pK}_a) + 23.06E_{\text{red}} + C \quad (1)$$

Received: August 2, 2016

Published: September 9, 2016

As shown in Figure 1, each reported acid-reductant combination used in catalytic ammonia synthesis generates a

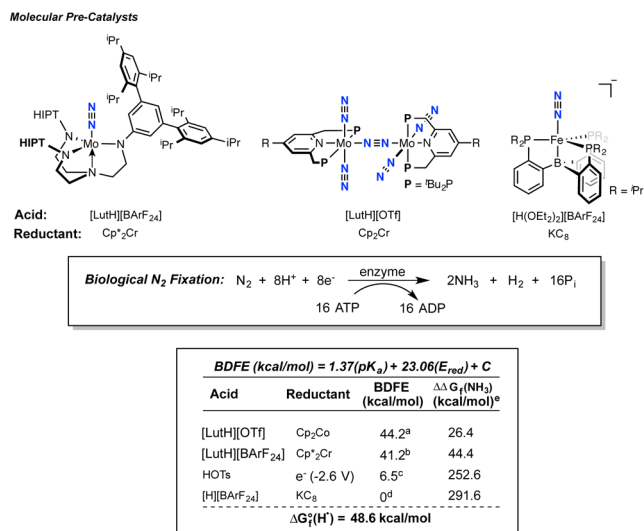


Figure 1. (Top) Molecular catalysts for reduction of N₂ to NH₃ using sources of protons and electrons. (Bottom) Effective BDFE values for various acid/reductant combinations and calculated overpotentials for NH₃ formation. ^apK_a (MeCN) = 14.4, E_{red} (vs Fc/Fc⁺) = -1.32 V. ^bpK_a (MeCN) = 14.4, E_{red} (vs Fc/Fc⁺) = -1.45 V. ^cpK_a (MeCN) = 8.4, E_{red} (Hg-pool cathode, vs Fc/Fc⁺) = -2.6 V. ^dpK_a (Et₂OH⁺, DMSO) = -3.2, E_{red} (vs Fc/Fc⁺) estimated as -3.0 V. ^eChemical overpotential calculated as 6(48.6-BDFE).

relatively weak effective BDFE and hence high chemical overpotential for each of these reagents. Likewise, nitrogenase enzymes, by virtue of the stoichiometry of the catalytic reaction requiring eight protons and electrons coupled with consumption of 16 equiv of ATP operates with an estimated overpotential of 117 kcal/mol.¹² While current molecular catalysts are triumphs of chemical synthesis, coordination chemistry, ligand design and illustrate the sophistication within reach of homogeneous catalysis, they also highlight a fundamental challenge with using molecular catalysts for ammonia synthesis—strong acids and reductants are not necessarily good mimics of H₂. Nevertheless, successful molecular catalysts with molybdenum, iron and cobalt have been described for ammonia synthesis using combinations of strong acids and reductants as the source of N–H bonds.¹³ Eq 1 can be applied to specific acids and reductants and allows computation of an *effective* bond dissociation free energy (BDFE) for each combination in a given solvent.¹⁴

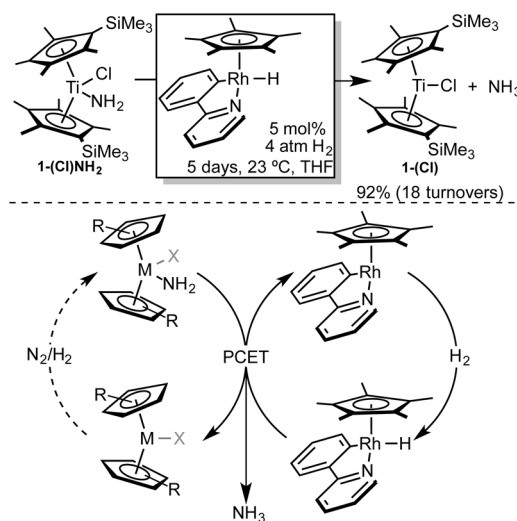
From a thermodynamic perspective, efficient nitrogen fixation occurs when the effective BDFE of the acid-reductant pair approaches the gas phase free energy value of the hydrogen atom, H[•] ($\Delta G_f^\circ(\text{H}^\bullet) = 48.6$ kcal/mol). In systems where the effective BDFE of an acid-reductant pair exhibit modest deviations from 48.6 kcal/mol, it is useful to calculate a *chemical overpotential* defined as $\Delta\Delta G_f(\text{NH}_3)$. This value is often significant and ranges between 29.6 and 291.6 kcal/mol for the reagents used with known molecular nitrogen fixation catalysts. Such an analysis highlights the challenge of using strong external acids and reductants for N₂ fixation and underscores the unique role of dihydrogen as the most energy efficient source of protons and electrons. Unfortunately treatment of molecular dinitrogen compounds with H₂ often leads to N₂ displacement,¹⁶ in rare instances where the

dinitrogen ligand is sufficiently activated, N₂ hydrogenation to form N–H bonds has been observed.^{17,18} However, strong acids or potent electrophiles are often required to remove the functionalized nitrogen ligand from the coordination sphere of the transition metal and the conditions are typically incompatible with catalytic turnover.^{19,20}

Release of coordinated nitrogen ligands to free ammonia or hydrazine is anticipated to be thermodynamically favored; it is the high kinetic barrier that limits reactivity. As a consequence, proton coupled electron transfer (PCET) and related hydrogen atom transfer (HAT) reactions are attractive alternatives for ammonia synthesis by hydrogenation as reaction trajectories may be accessed that avoid high-energy intermediates and open an energetically accessible pathway for product release.²¹ It is possible that the known molecular molybdenum catalysts reported by Schrock and Nishibayashi that rely on a pyridinium acid and metallocene reductants, operate by PCET or HAT²² as pyridinyl radicals are known to have relatively weak N–H bonds (BDFE \approx 35 kcal/mol).²³

Our laboratory has recently reported the application of PCET to catalytic ammonia synthesis via hydrogenation by treatment of a titanocene(IV) amide complex with (η^5 -C₅Me₅) (py-Ph)RhH ([Rh]-H; py-Ph = 2-pyridylphenyl),²⁴ a compound first described by Norton and co-workers (Scheme 1).²⁵

Scheme 1. (Top) Catalytic Hydrogenolysis of a Ti–N Bond Resulting in the Formation of a Reduced Titanium Complex and Free Ammonia; (Bottom) Hypothetical Scheme for the Catalytic Formation of NH₃ via PCET Mediated by a Rhodium Cocatalyst



During the course of these investigations, rare experimental measures of N–H BDFEs were obtained for the addition of a hydrogen atom to parent amido (M–NH₂) ligands in a family of group 4 metallocene complexes.²⁶ Hydrogenation of the Ti–NH₂ bond does not occur in the absence of rhodium hydride catalyst, highlighting both the high kinetic barrier of the background reaction and the utility of the PCET-HAT approach.

Key to expanding these initial observations into a general method for ammonia synthesis and breaking otherwise strong bonds to transition metals is obtaining a thorough understanding of the BDFEs of the N–H bonds in various coordinated nitrogen ligands—particularly diazenides, imides and amides found along the N₂ fixation cycle. While PCET has

been implied in a number of examples,²⁷ detailed thermodynamic bracketing and estimation of thermochemical parameters for N–H bond formation and cleavage is rare and has typically been confined to metal imido and nitrido species.²⁸ A systematic body of experimentally determined N–H BDFEs as a function of type of nitrogen ligand (nitride, imide, amide, ammine), metal, and supporting ligand is currently absent from the literature and would provide useful guiding principles for rational catalyst design. Here we describe a systematic study of PCET with a series of titanocene and zirconocene complexes bearing imide, hydrazide and amide ligands and describe the mechanistic and thermodynamic parameters for productive N–H bond formation. Two structurally and thermodynamically distinct metal hydrides were explored and experimental and computational data for N–H BDFEs in 12 different complexes along a hypothetical nitrogen fixation cycle are also reported.

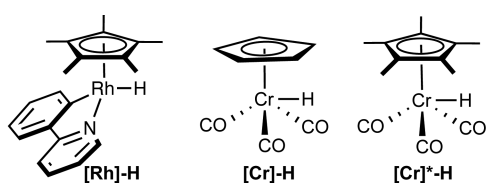
RESULTS AND DISCUSSION

The identity and thermodynamic properties of the hydrogen atom transfer reagent are essential for enabling successful PCET for N–H bond formation to a nitrogen-containing ligand. Detailed thermochemical properties, typically represented as thermochemical square schemes, provide the means for determining the overall thermodynamics of a PCET reaction and the extent to which proton transfer and electron transfer are anticipated to be coupled.^{21,29} To realize catalytic PCET where the protons and electrons are ultimately derived from H₂, transition metal compounds capable of promoting catalytic homolytic H₂ cleavage followed by net atom transfer to form an N–H bond were evaluated.

[Rh]-H was an excellent starting point for these studies due to its ease of synthesis, the availability of sound thermochemical data²⁴ and proven capability in the catalytic hydrogenation of TEMPO• (2,2,6,6-tetramethylpiperidine 1-oxyl), and titanocene amides to release free ammonia. The chromium hydride, ($\eta^5\text{-C}_5\text{H}_5$)(CO)₃CrH ([Cr]-H)³⁰ was also of interest due to its well established thermodynamic properties³¹ and its known compatibility with sensitive and reactive group 4 metallocenes. Norton³² and others³³ have also demonstrated [Cr]-H as a catalyst for radical cyclization and hydrogenation reactions that proceed via PCET. Rational modifications of the cyclopentadienyl ligand in [Cr]-H also modulate the thermochemical properties, solubility and crystallinity with ($\eta^5\text{-C}_5\text{Me}_5$)(CO)₃CrH ([Cr]*-H) serving as the most well-known example.³⁴ Table 1 reports the thermochemical properties for [Rh]-H, [Cr]-H, and [Cr]*-H. Although gas-phase [M]-H BDFEs have been calculated and reported previously,^{32c} the values listed in Table 1 have been recalculated for consistency with other calculated BDFE values reported in this work.

There are a number of important aspects to note concerning the similarities and differences between [Rh]-H, [Cr]-H, and [Cr]*-H. The most obvious distinction is the dramatic change in the acidity of the three metal hydrides with both [Cr]-H, and [Cr]*-H being more than 10 orders of magnitude more acidic than [Rh]-H. The [M]^{0/-} redox couple for the chromium complexes are anodically shifted by approximately 1 V compared to [Rh]-H. Comparing [Cr]-H to [Cr]*-H, [Cr]*-H is more basic by 3 pK_a units and more reducing 140 mV, consistent with expectations from permethylation of the cyclopentadienyl ring. Importantly, the reduced acidity and cathodic shift offset and there is no significant change in the overall [M]-H BDFE between the two chromium compounds.

Table 1. Thermochemical Data for the Metal Hydrides Used in This Study



	[Rh]-H	[Cr]-H	[Cr]*-H
pK _a ^a	30.3 (20.2) ^e	13.3 (7.8) ^g	16.1 (10.1) ^g
E _{red} (V) ^b	-1.85 (-1.98) ^f	-0.69 (-0.67) ^g	-0.83 (-0.83) ^g
BDFE (exp) ^c	52.3 kcal/mol	57.3 kcal/mol	57.8 kcal/mol
BDFE (calc) ^d	55 kcal/mol	52 kcal/mol	53 kcal/mol

^apK_as are reported in MeCN solvent and THF (italicized). ^bE_{red} reported for the [M]^{0/-} couple in MeCN and THF (italicized) vs Fc/Fc⁺. ^cCalculated in MeCN solvent using eq 1 with C = 54.9 kcal/mol²¹. ^dDFT calculated gas-phase BDFE. See Supporting Information for details. ^eIn MeCN solution the phosphazene base (*tert*-butylimino)-tris(pyrrolidino)phosphorane was required to deprotonate [Rh]-H. The pK_a of this base in THF is 20.2.²⁴ ^fSee ref 24. ^gSee ref 31 for values in MeCN. Values in THF have been redetermined (see text).

The calculated and experimentally determined BDFE values for all three metal hydride compounds are in the range of 50–60 kcal/mol. Assuming that the theoretical minimum value for a hydrogen atom donor derived from H₂ is equal to the free energy of formation of H• (48.6 kcal/mol), [M]-H BDFEs higher than 48.6 kcal/mol decrease the thermodynamic feasibility of the hypothetical catalytic cycle shown in Scheme 1. As such, [Rh]-H is a more desirable hydrogen atom donor than [Cr]-H and [Cr]*-H. However, thermodynamic assessment of the relative bond strengths alone may not be an accurate predictor of reactivity as kinetic preferences may dominate.

Our studies on PCET as applied to N–H bond formation relevant to nitrogen fixation commenced with titanocene compounds. This platform was chosen due to the historical significance of titanium complexes to ammonia synthesis,³⁵ the expected chemical inertness and modularity of the cyclopentadienyl ligands and the ability of sterically hindered metallocene environment to support rare examples of monomeric imides, hydrazides and amides in some cases in different oxidation states.

The titanocene(III) *N,N*-dimethyl hydrazide(–1) compound, ($\eta^5\text{-C}_5\text{Me}_4\text{SiMe}_3$)₂TiNHNMe₂ (1-NHNMe₂), was prepared by straightforward salt metathesis by treatment of ($\eta^5\text{-C}_5\text{Me}_4\text{SiMe}_3$)₂TiCl (1-Cl) with LiNHNMe₂. Oxidation of this compound by chlorine atom transfer with (C₆H₅)₃CCl cleanly yielded the related chloride derivative, ($\eta^5\text{-C}_5\text{Me}_4\text{SiMe}_3$)₂Ti(Cl)NHNMe₂ (1-(Cl)NHNMe₂). Representations of the solid state structures of both compounds are presented in Figure 2 and establish rare κ^1 coordination³⁶ of the hydrazide(–1) ligand. The majority of titanium hydrazide(–1) complexes exhibit side-on κ^2 coordination³⁷ and serve to highlight the unique steric environment imparted by the substituted cyclopentadienyl ligands. Importantly the κ^1 coordination mode allows for more direct analogies to be drawn to 1-NH₂ and 1-(Cl)NH₂ in subsequent thermochemical studies. Attempts to prepare ($\eta^5\text{-C}_5\text{Me}_4\text{SiMe}_3$)₂TiNHNH₂ (1-NHNH₂) and ($\eta^5\text{-C}_5\text{Me}_4\text{SiMe}_3$)₂Ti(Cl)NHNH₂ (1-(Cl)NHNH₂) by analogous methods to the syntheses of 1-NHNMe₂ and 1-(Cl)NHNMe₂ were unsuccessful, yielding mixtures of unidentifiable titanium products.

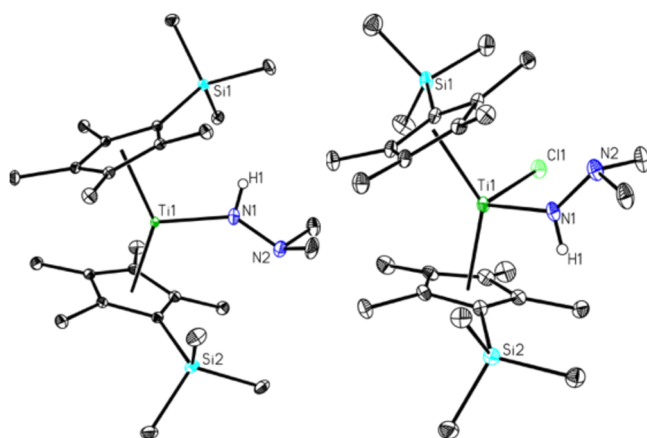


Figure 2. ORTEP representations of the solid state structures of **1-NHNMe₂** (left) and **1-(Cl)NHNMe₂** (right) at 30% probability ellipsoids. Hydrogen atoms, except those attached to N(1), have been omitted for clarity.

To gain insight into the PCET N–H bond forming reactivity of complexes with titanium–nitrogen multiple bonds, the titanium imido compound ($\eta^5\text{-C}_5\text{Me}_4\text{SiMe}_3$)₂TiNSiMe₃ (**1=NSiMe₃**) was prepared. Our group previously reported the reactivity of **1=NSiMe₃** with H₂ and described facile 1,2 addition to form ($\eta^5\text{-C}_5\text{Me}_4\text{SiMe}_3$)₂Ti(H)NHSiMe₃ (**1-(H)-NHSiMe₃**).³⁸ However, the thermochemistry of **1=NSiMe₃** relevant to PCET was not examined. Additionally, **1-(H)-NHSiMe₃** proved unreactive toward H₂ and did not release free silylamine.

With this family of compounds in hand, the viability of catalytic PCET with H₂ and catalytic [Rh]-H, [Cr]-H and [Cr]*-H were evaluated (Table 2). Each experiment was conducted with 5 mol % of [Rh]-H and 10 mol % of each of the chromium reagents, [($\eta^5\text{-C}_5\text{H}_5$) (CO)₃Cr]₂ ([Cr]₂) and [($\eta^5\text{-C}_5\text{Me}_5$) (CO)₃Cr]₂ ([Cr]*₂). Hydrogenation of the dimeric chromium precursors yielded [Cr]-H and [Cr]*-H producing a final loading of 20 mol % in each case. Each reaction was stirred for 5 days and following vacuum transferring of the volatiles, was analyzed for ammonia by the indophenol method³⁹ (entries 1–11) or NH₂NMe₂ by quantitative ¹H NMR spectroscopy (entries 12–15). For each entry, a corresponding control reaction without catalyst was performed; in all controls, the formation of NH₃ or NH₂NMe₂ was not observed.

As was previously reported, [Rh]-H is a competent catalyst for the hydrogenolysis of the amide ligand in **1-(Cl)NH₂** (entry 1, 92% NH₃, TON = 18) but not in **1-NH₂** or ($\eta^5\text{-C}_5\text{Me}_4\text{SiMe}_3$)₂Zr(Cl)NH₂ (**2-(Cl)NH₂**) (entries 4 and 7, 0% NH₃).²⁴ Repeating the hydrogenation of **1-(Cl)NH₂** with [Cr]-H or [Cr]*-H (entries 2–3) produced only 37% NH₃ (TON = 1.9) and 34% NH₃ (TON = 1.7), respectively, despite the higher catalyst loading compared to [Rh]-H. Although the apparent yields of NH₃ are low, the observation of TONs greater than 1 indicate that [Cr]-H and [Cr]*-H are regenerated under catalytic conditions. The reactions of [Cr]-H and [Cr]*-H with **1-NH₂** and **2-(Cl)NH₂** (entries 5–6, 8–9) yielded 15–19% NH₃ (TON: 0.85–0.95), establishing stoichiometric reactivity between the chromium reagents and the metal amides.

The titanium imido complex, **1=NSiMe₃**, was completely consumed in the presence of 5 mol % of [Rh]-H under 4 atm of H₂ (entry 10). Analysis of the volatiles by ¹H NMR

Table 2. Catalytic Hydrogenolysis of Various Complexes Using Metal Hydride Reagents in the Presence of 4 atm H₂

entry	complex	[M-H] ^a	NR ₂ -H ^b	TON (NR ₂ H/[Cat]) ^c
1	1-(Cl)NH₂	[Rh]	92	18
2		[Cr]	37	1.9
3		[Cr]*	34	1.7
4	1-NH₂	[Rh]	0	0
5		[Cr]	17	0.85
6		[Cr]*	19	0.95
7	2-(Cl)NH₂	[Rh]	0	0
8		[Cr]	18	0.90
9		[Cr]*	15	0.75
10	1=NSiMe₃	[Rh]	95	19
11		[Cr]	36	1.8
12	1-(Cl)NHNMe₂	[Rh]	87	17
13		[Cr]	33	1.7
14	1-NHNMe₂	[Rh]	0	0
15		[Cr]	15	0.75

^a[Rh] = ($\eta^5\text{-C}_5\text{Me}_5$) (py-Ph)RhH, 5 mol %. [Cr] = [($\eta^5\text{-C}_5\text{H}_5$)Cr(CO)₃]₂, 10 mol %. [Cr]* = [($\eta^5\text{-C}_5\text{Me}_5$)Cr(CO)₃]₂, 10 mol %. ^bDetermined by spectrophotometry (entries 1–11) and quantitative ¹H NMR (entries 12–15). ^cCalculated as the number of moles of NR₂H divided by the number of moles of monomeric metal hydride.

spectroscopy established formation of H₂NSiMe₃. Quantitation by the indophenol method following hydrolysis to ammonia established near quantitative (>95%) formation of NH₃, demonstrating successful catalytic hydrogenolysis of a titanium nitrogen double bond with a TON of 19 with the [Rh]-H catalyst. Repeating the hydrogenation of **1=NSiMe₃** with 20 mol % [Cr]-H (entry 11) produced a different outcome with a 36% yield of H₂NSiMe₃ (quantified as NH₄Cl) corresponding to a TON of 1.8. While observation of a TON greater than 1 is consistent with PCET from [Cr]-H followed by catalyst regeneration. The dramatically reduced efficiency of [Cr]-H compared to [Rh]-H is notable and suggests that the two catalysts may operate by different mechanisms.

The catalytic hydrogenolysis of the titanium hydrazido complexes, **1-NHNMe₂** and **1-(Cl)NHNMe₂**, was also explored. The observed reactivity paralleled the chemistry observed with **1-(Cl)NH₂** and **1-NH₂**; treatment of **1-(Cl)NHNMe₂** with 5 mol % [Rh]-H under 4 atm of H₂ yielded 87% H₂NNMe₂ (TON = 17). However, H₂NNMe₂ was not observed when the Ti(III) hydrazide, **1-NHNMe₂**, was subjected to catalytic conditions. When 20 mol % [Cr]-H was employed as the hydrogen atom donor, **1-(Cl)NH₂NMe₂** afforded 33% H₂NNMe₂ (TON = 1.7) while **1-NHNMe₂** afforded substoichiometric quantities of NH₂NMe₂ (15%, TON = 0.75).

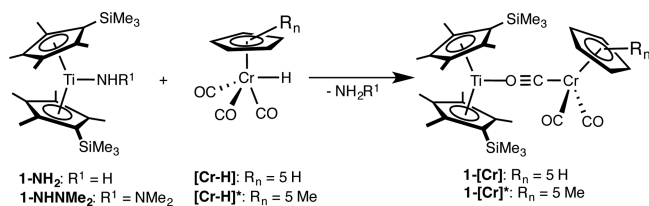
The data in Table 2 establishes important trends for hydrogenolysis of titanium–nitrogen bonds by proton coupled electron transfer. All of the titanium(IV) compounds underwent catalytic Ti–N hydrogenolysis (TON > 1) using [Rh]-H, [Cr]-H, and [Cr]*-H. Among these, [Rh]-H was the most

efficient hydrogen atom donor (TONs ≈ 20), supporting a pathway involving PCET from $[\text{Rh}]\text{-H}$ to the Ti-NR_2 ligand followed by regeneration of the metal-hydride from activation of H_2 by the resulting metalloradical. By comparison, $[\text{Cr}]\text{-H}$ and $[\text{Cr}]^*\text{-H}$ are inefficient hydrogen atom donors (TONs ≈ 2), though observation of TONs greater than 1 indicates catalytic regeneration of the metal hydrides. All Ti(III) compounds proved unreactive toward $[\text{Rh}]\text{-H}$ and hydrogenolysis products were not detected. However, when $[\text{Cr}]\text{-H}$ and $[\text{Cr}]^*\text{-H}$ were used, variable amounts of product were formed from the Ti(III) complexes. Importantly, the low yields of NR_2H (TONs < 1) demonstrate stoichiometric rather than catalytic reactions between the chromium hydrides and the Ti(III) complexes with little to no regeneration of the metal hydride catalyst.

To gain insight into poor catalytic efficiency of $[\text{Cr}]\text{-H}$ and $[\text{Cr}]^*\text{-H}$ compared to $[\text{Rh}]\text{-H}$, a series of stoichiometric studies were performed. Given the similar reactivity of $[\text{Cr}]^*\text{-H}$ and $[\text{Cr}]\text{-H}$ under catalytic conditions and their similar thermochemical properties (Table 1), the two compounds were used interchangeably in these experiments and were selected based on the ability to observe or isolate relevant intermediates.

Initial stoichiometric studies comparing metal reagents were conducted using 1-NH_2 (Scheme 2). Addition of $[\text{Cr}]^*\text{-H}$ to a

Scheme 2. Reactivity of a Ti(III) Amide and a Ti(III) Hydrazide (–1) with Chromium Hydride Reagents



toluene solution of 1-NH_2 resulted in an immediate color change from purple to red. The volatile products were analyzed by the indophenol method, establishing formation of ammonia in 91% yield. The organometallic product of the reaction was identified as the $S = 1/2$ ($\mu_{\text{eff}, 23^\circ\text{C}} = 1.7 \mu\text{B}$) titanocene, $(\eta^5\text{-C}_5\text{Me}_4\text{SiMe}_3)_2\text{Ti}(\mu\text{-CO})\text{Cr}(\text{CO})_2(\eta^5\text{-C}_5\text{Me}_5)$ (1-[Cr]^*) as determined by single crystal X-ray diffraction (Figure 3). The presence of a chromium carbonyl subunit in the product was confirmed by infrared spectroscopy with observation of a strong and diagnostic band centered at 1638.7 cm^{-1} . This band was successfully reproduced by full molecule DFT calculations, where a vibrational mode was identified at 1620 cm^{-1} , assigned as the $\mu\text{-CO}$ stretch.

The room temperature X-band EPR spectrum of 1-[Cr]^* in toluene displays a single feature at $g_{\text{iso}} = 1.974$ with a hyperfine interaction to the ^{47}Ti nucleus ($I = 5/2$, $A_{\text{iso}} = 49.3 \text{ MHz}$). No ^{53}Cr (9.5%, $I = 3/2$) hyperfine was observed, consistent with a titanium-based SOMO. This view of the electronic structure was also confirmed by DFT calculations where spin density was located principally on the titanium (see Figure S14).

Similar reactivity was observed with 1-NHNMe_2 (Scheme 2). Addition of $[\text{Cr}]^*\text{-H}$ to a toluene solution of 1-NHNMe_2 resulted in an immediate color change from purple to red. The volatiles of the reaction were analyzed by ^1H NMR spectroscopy using 1,3,5-trimethoxybenzene as an internal reference and found to contain NH_2NMe_2 (76%). Analysis of the

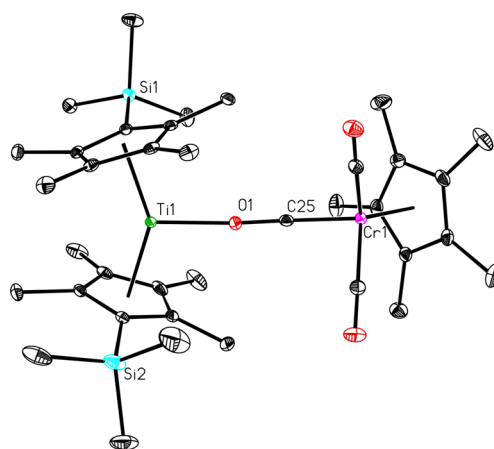


Figure 3. ORTEP representations of the solid-state structures of 1-[Cr]^* at 30% probability ellipsoids. Hydrogen atoms have been omitted for clarity.

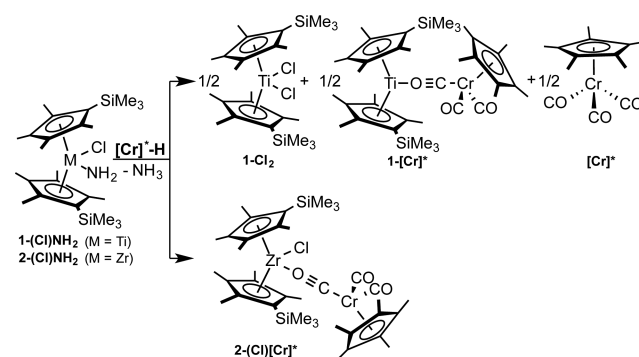
nonvolatile organometallic residue by EPR spectroscopy identified the concomitant formation of 1-[Cr]^* and the featureless NMR spectrum confirmed no other byproducts.

Reaction of both 1-NH_2 and 1-NHNMe_2 with $[\text{Cr}]^*\text{-H}$ are best viewed as straightforward protonations with release of ammonia or substituted hydrazine with concomitant capture of the chromium anion by titanium. Because the titanium remains in the +3 oxidation state both before and after the reaction, proton transfer is facile but electron transfer does not occur.

Thermochemical measurements were conducted to understand the lack of electron transfer reactivity. The pK_a of $[(\eta^5\text{-C}_5\text{Me}_4\text{SiMe}_3)_2\text{Ti}(\text{NH}_3)][\text{BAR}^{\text{F}_4}]$ ($[\text{1-NH}_3]^+$) was previously determined as 16.2 in THF.²⁴ Although the pK_a of $[\text{Cr}]^*\text{-H}$ in CH_3CN is reported at 16.1, this value has been redetermined in THF by equilibration with collidinium ($\text{pK}_a = 8.1$) and 1,8-bis(dimethylamino)naphthalene (“DMAN”, $\text{pK}_a = 11.1$)⁴⁰ and found to be 10.1. Thus, in the reaction medium (THF), $[\text{Cr}]^*\text{-H}$ is 6 orders of magnitude more acidic than $[\text{1-NH}_3]^+$. The redox potential of the $[\text{Cr}]^{*(0/-)}$ couple was also redetermined in THF solution as -0.83 V .⁴¹ Because the $\text{Ti(III)}/\text{Ti(II)}$ redox couple for $[\text{1-NH}_3]^{+/0}$ is -2.0 V ,⁴² electron transfer from $\{[\text{Cr}]^*\}^-$ to $[\text{1-NH}_3]^+$ is highly endergonic while proton transfer is highly exergonic. As a result, protonation but not electron transfer occurs.

The stoichiometric reactivity of $[\text{Cr}]^*\text{-H}$ with 1-(Cl)NH_2 and 2-(Cl)NH_2 was also examined (Scheme 3). Addition of $[\text{Cr}]^*\text{-H}$ to a toluene solution of 2-(Cl)NH_2 resulted in an

Scheme 3. Divergent Reactivity of 1-(Cl)NH_2 and 2-(Cl)NH_2 with $[\text{Cr}]^*\text{-H}$



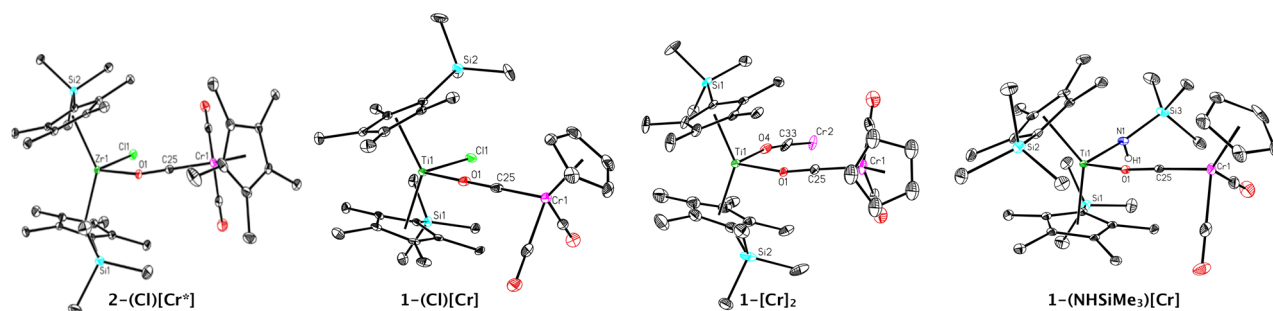
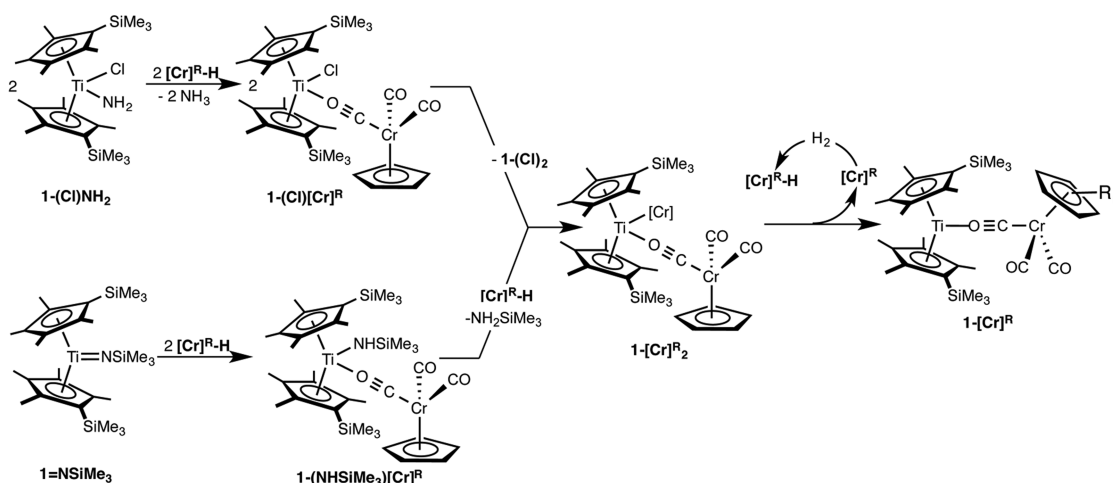


Figure 4. ORTEP representations of the solid state structures of mechanistically relevant heterobimetallic complexes. Left to right: $2-(\text{Cl})[\text{Cr}]^*$, $1-(\text{Cl})[\text{Cr}]$, $1-[\text{Cr}]_2$, $1-(\text{NHSiMe}_3)[\text{Cr}]$. Hydrogen atoms except that attached to N1 have been omitted for clarity.

Scheme 4. Proposed Reaction Pathway That Accounts for the Formation of NH_3 and the Pseudocatalytic Regeneration of Chromium Hydride Reagents under H_2



immediate color change from colorless to deep red. Analysis of the volatile products of the reaction established 93% formation of NH_3 while analysis of the nonvolatile organometallic components established formation of the C_5 symmetric zirconocene, $(\eta^5\text{-C}_5\text{Me}_4\text{SiMe}_3)_2\text{Zr}(\text{Cl})(\mu\text{-CO})\text{Cr}(\text{CO})_2(\eta^5\text{-C}_5\text{Me}_5)$ ($2-(\text{Cl})[\text{Cr}]^*$, 89%). This product was identified by a combination of X-ray diffraction (Figure 4) and by solid-state (KBr) infrared spectroscopy, which exhibits a diagnostic band at 1530.4 cm^{-1} . This feature was assigned as a bridging carbonyl based on DFT frequency calculations ($\nu_{\text{DFT}} = 1545\text{ cm}^{-1}$). As expected based on the data in Table 2, $2-(\text{Cl})[\text{Cr}]^*$ was unreactive toward H_2 , consistent with the observation that $[\text{Cr}]^*\text{-H}$ was not regenerated. The $\text{p}K_{\text{a}}$ of $[(\eta^5\text{-C}_5\text{Me}_4\text{SiMe}_3)_2\text{Zr}(\text{Cl})(\text{NH}_3)][\text{BAR}^{\text{F}}_4]$ ($[2-(\text{Cl})\text{NH}_3]^+$) in THF was previously determined as 14.7 indicating that the protonation of $2-(\text{Cl})\text{NH}_2$ by $[\text{Cr}]^*\text{-H}$ is highly favored. The $\text{Zr}(\text{IV})/\text{Zr}(\text{III})$ redox couple for $[2-(\text{Cl})\text{NH}_3]^{(+/0)}$ is -2.0 V , making subsequent electron transfer from $\{[\text{Cr}]^*\}^-$ energetically inaccessible. Analogous to 1-NH_2 , PCET from $[\text{Cr}]^*\text{-H}$ to $2-(\text{Cl})\text{NH}_2$ is thermodynamically inaccessible while stoichiometric protonation is facile.

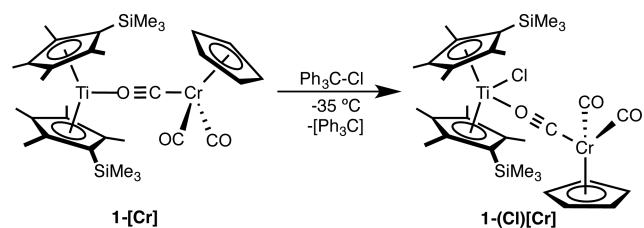
The reactivity of $[\text{Cr}]^*\text{-H}$ with $1-(\text{Cl})\text{NH}_2$ exhibited more complex behavior (Scheme 3). Upon addition of $[\text{Cr}]^*\text{-H}$ to a benzene- d_6 solution containing $1-(\text{Cl})\text{NH}_2$ and 1,3,5-trimethoxybenzene as an internal standard, an immediate color change from yellow to dark red was observed. Analysis by ^1H NMR spectroscopy established formation $(\eta^5\text{-C}_5\text{Me}_4\text{SiMe}_3)_2\text{TiCl}_2$ ($1-(\text{Cl})_2$) in 42% yield. The volatiles of the reaction were analyzed by NMR spectroscopy and 83% of

the expected NH_3 was identified. Exposure of a benzene- d_6 solution of the nonvolatile products to 4 atm of H_2 resulted in regeneration of $[\text{Cr}]^*\text{-H}$ in 46% yield. In a separate reaction, the nonvolatile products were analyzed by IR spectroscopy and exhibited spectroscopic signatures diagnostic with the formation of $1-[\text{Cr}]^*$. The observed reaction products can be rationalized by the following sequence shown in Scheme 4: (i) initial protonation of $1-(\text{Cl})\text{NH}_2$ by $[\text{Cr}]^*\text{-H}$ to yield the putative bimetallic intermediate, $(\eta^5\text{-C}_5\text{Me}_4\text{SiMe}_3)_2\text{Ti}(\text{Cl})(\mu\text{-CO})\text{Cr}(\text{CO})_2(\eta^5\text{-C}_5\text{Me}_5)$ ($1-(\text{Cl})[\text{Cr}]^*$); (ii) ligand redistribution from $1-(\text{Cl})[\text{Cr}]^*$ to form $(\eta^5\text{-C}_5\text{Me}_4\text{SiMe}_3)_2\text{Ti}[(\mu\text{-CO})\text{Cr}(\text{CO})_2(\eta^5\text{-C}_5\text{Me}_5)]_2$ ($1-[\text{Cr}]^*_2$) and $1-(\text{Cl})_2$; and (iii) disproportionation of $1-[\text{Cr}]^*_2$ to $1-[\text{Cr}]^*$ and $[\text{Cr}]^*$. The formation of $[\text{Cr}]^*$, a molecule that forms $[\text{Cr}]^*\text{-H}$ upon treatment with H_2 , explains the pseudocatalytic behavior observed in Table 2. However, generation of 0.5 equiv of $1-[\text{Cr}]^*$ per molecule of NH_3 limits the overall catalytic performance to two turnovers. This reaction sequence also explains the observation of turnover numbers approaching 2 for the reactions of $1-(\text{Cl})\text{NH}_2$ and $1-(\text{Cl})(\text{NHNMe}_2)$ with $[\text{Cr}]^*\text{-H}$ and $[\text{Cr}]^*\text{-H}$ under catalytic conditions.

To support to the reaction sequence proposed in Scheme 4, direct evidence for the formation of $1-(\text{Cl})[\text{Cr}]^*$ was sought. Addition of Ph_3CCl as a potential chlorine atom donor to $1-[\text{Cr}]^*$ instead resulted in formation of a mixture of $1-\text{Cl}_2$ and $1-[\text{Cr}]^*$ as judged by ^1H NMR spectroscopy and decomposition studies. It is likely that the sterically encumbered pentamethylcyclopentadienyl ligand contributes to the observed instability of $1-(\text{Cl})[\text{Cr}]^*$ and ligand redistribution results.

To support this hypothesis, the chlorination procedure was repeated with 1-[Cr] in place of 1-[Cr]^* (Scheme 5). Addition

Scheme 5. Low Temperature Reaction of 1-[Cr] with $(\text{C}_6\text{H}_5)_3\text{CCl}$ ($\text{Ph}_3\text{C-Cl}$) to Afford the Thermally Unstable Complex, 1-Cl[Cr]



of $(\text{C}_6\text{H}_5)_3\text{CCl}$ to a concentrated pentane solution of 1-[Cr] at $-35\text{ }^\circ\text{C}$ followed by solvent evaporation resulted in isolation of red crystals of $(\eta^5\text{-C}_5\text{Me}_4\text{SiMe}_3)_2\text{Ti}(\text{Cl})(\mu\text{-CO})\text{Cr}(\text{CO})_2(\eta^5\text{-C}_5\text{H}_5)$, 1-Cl[Cr] .

The solid state structure of 1-Cl[Cr] was determined by X-ray diffraction (Figure 4) and the overall coordination geometry is typical of a bent metallocene and is structurally analogous to $(\eta^5\text{-C}_5\text{Me}_5)_2\text{Ti}(\text{CH}_3)(\mu\text{-CO})\text{Mo}(\text{CO})_2(\eta^5\text{-C}_5\text{H}_5)$, reported by Stucky and co-workers from the reaction of $(\eta^5\text{-C}_5\text{Me}_5)(\eta^6\text{-C}_5\text{Me}_4\text{CH}_2)\text{Ti}(\text{CH}_3)$ with $(\eta^5\text{-C}_5\text{H}_5)(\text{CO})_3\text{MoH}$.⁴³ A diagnostic solid-state infrared band was observed at 1602.7 cm^{-1} , a value successfully reproduced ($\nu_{\text{CO}} = 1598\text{ cm}^{-1}$) by the DFT computed frequency spectrum and assigned as the $\mu\text{-CO}$ stretching mode. In benzene solution, 1-Cl[Cr] proved unstable with respect to ligand redistribution, converting to a mixture of 1-Cl_2 , 1-[Cr] , and $[\text{Cr}]_2$ over the course of minutes at $23\text{ }^\circ\text{C}$ as determined by a combination of ^1H NMR and IR spectroscopies as well as decomposition studies. Attempts to obtain the ^1H NMR spectrum and elemental analysis of 1-Cl[Cr] have been unsuccessful due to this instability. Nevertheless, the observation of 1-Cl[Cr] and the instability of both 1-Cl[Cr]^* and 1-Cl[Cr] with respect to ligand redistribution and disproportionation supports the hypothesis that these compounds are intermediates on the route to the regeneration of $[\text{Cr}]^*\text{-H}$ and $[\text{Cr}]\text{-H}$, as shown in Scheme 4.

The observed reactivity of 1-ClNH_2 with $[\text{Cr}]^*\text{-H}$ is an instructive example for application of proton coupled electron transfer to N_2 functionalization. The BDFEs for $[\text{Cr}]^*\text{-H}$ (60.7 kcal/mol) and 1-ClNH_3 (61.2 kcal/mol) in THF suggests that PCET from $[\text{Cr}]^*\text{-H}$ to the titanocene amide ligand should be thermodynamically feasible. However, the thermochemical properties of the chromium hydride reveal that ΔG for proton transfer is -6.7 kcal/mol while ΔG for subsequent electron transfer is $+6.2\text{ kcal/mol}$.⁴² A similar analysis holds for the reaction with $[\text{Cr}]\text{-H}$ ($\Delta G_{\text{PT}} = -9.9\text{ kcal/mol}$; $\Delta G_{\text{ET}} = 9.9\text{ kcal/mol}$). Therefore, ammonia release via protonation and formation for 1-Cl[Cr]^* is the preferred reaction pathway. In examining the thermochemistry for the reaction of 1-ClNH_2 with $[\text{Rh}]\text{-H}$ in THF, ΔG for the proton transfer is 7.1 kcal/mol while ΔG for subsequent electron transfer is -20.3 kcal/mol . Thus, the thermodynamic trap arising from a highly exergonic protonation step is operative for $[\text{Cr}]\text{-H}$ but not for $[\text{Rh}]\text{-H}$.

This comparison highlights the importance of the hydrogen atom donor and the hydrogen atom acceptor to have both ΔpK_a and $\Delta E^{1/2}$ properly matched to avoid thermodynamically favored side reactions. The experimental observation of

pseudocatalytic regeneration of $[\text{Cr}]^*\text{-H}$ is likely a result of the instability of 1-Cl[Cr]^* with respect to the formation of 1-[Cr]^* . The two π -acidic $\mu\text{-CO}$ ligands coordinated to the Ti center in 1-[Cr]^* would be expected to attenuate the otherwise inaccessible Ti(IV)/Ti(III) reduction potential and thus allow for electron transfer from the chromium anion and formation of 1-[Cr]^* and $[\text{Cr}]^*$ (Scheme 4).

The stoichiometric reactivity of 1=NSiMe_3 with $[\text{Cr}]\text{-H}$ was also examined because of the observed TON of 1.8 under catalytic conditions. Addition of $[\text{Cr}]\text{-H}$ to a pentane solution 1=NSiMe_3 resulted in a color change from red to orange. Slow evaporation of this solution over 6 h furnished crystals suitable for X-ray diffraction in 75% yield. The solid-state structure of $(\eta^5\text{-C}_5\text{Me}_4\text{SiMe}_3)_2\text{Ti}(\text{NHSiMe}_3)(\mu\text{-CO})\text{Cr}(\text{CO})_2(\eta^5\text{-C}_5\text{H}_5)$ ($1\text{-NHSiMe}_3[\text{Cr}]$) established protonation of the imido fragment with subsequent coordination of the anionic chromium complex through a bridging $\mu\text{-CO}$ ligand. The ^1H NMR spectrum of $1\text{-NHSiMe}_3[\text{Cr}]$ exhibits the number of peaks consistent with C_s molecular symmetry with the N–H resonance located at 9.39 ppm. The KBr infrared spectrum exhibits medium and intensity band at 3320.0 cm^{-1} assigned to the N–H stretch while a stronger feature was observed at 1630.5 cm^{-1} for the $\mu\text{-CO}$ vibration. Isolated $1\text{-NHSiMe}_3[\text{Cr}]$ was unreactive toward 4 atm H_2 over a period of 5 days as neither formation of NH_2SiMe_3 nor $[\text{Cr}]\text{-H}$ was observed.

Addition of a second equivalent of $[\text{Cr}]\text{-H}$ to $1\text{-NHSiMe}_3[\text{Cr}]$ produced an unexpected outcome. Monitoring the reaction by ^1H NMR spectroscopy in the presence of 1,3,5-trimethoxybenzene as an internal standard revealed formation of NH_2SiMe_3 in 76% yield. No resonances for a diamagnetic titanium product were observed. Treatment of the mixture of NMR silent compounds with 4 atm of H_2 and analysis resulted in formation of $[\text{Cr}]\text{-H}$ in 42% yield as judged by ^1H NMR spectroscopy and integration versus the internal standard. In a separate reaction, an IR spectrum of the nonvolatile products prior to treatment with H_2 were collected and revealed a strong band at 1595.7 cm^{-1} (DFT calculated $\nu_{\text{CO}} = 1592\text{ cm}^{-1}$), consistent with the formation of 1-[Cr] . In an attempt to identify intermediates en route to formation of 1-[Cr] , the addition of two equivalents of $[\text{Cr}]\text{-H}$ to a concentrated pentane solution of 1=NSiMe_3 at $-35\text{ }^\circ\text{C}$ resulted in deposition of small crystals suitable for X-ray diffraction identified as $(\eta^5\text{-C}_5\text{Me}_4\text{SiMe}_3)_2\text{Ti}[(\mu\text{-CO})\text{Cr}(\text{CO})_2(\eta^5\text{-C}_5\text{H}_5)]_2$ (1-[Cr]_2) (Figure 4). The solid state structure of 1-[Cr]_2 contains two chromium fragments each with an isocarbonyl ligand coordinated to titanium. Full molecule DFT calculations support a titanium(IV) oxidation state assignment with two anionic isocarbonyl-linked chromium subunits (Figure S15). The solid-state KBr infrared spectrum of 1-[Cr]_2 exhibits two strong bands at 1607.4 and 1573.1 cm^{-1} . These are in good agreement with the calculated frequency spectrum, which predicts two bands corresponding to $\mu\text{-CO}$ stretching modes at 1590 and 1559 cm^{-1} . Attempts to obtain a ^1H NMR spectrum and elemental analysis of 1-[Cr]_2 were unsuccessful likely owing to the thermal instability of the compound.

EXPERIMENTAL BRACKETING AND CALCULATION OF N–H BDFES

Given the paucity of data on N–H BDFEs in coordination compounds^{24,26} and the importance of these values for rational

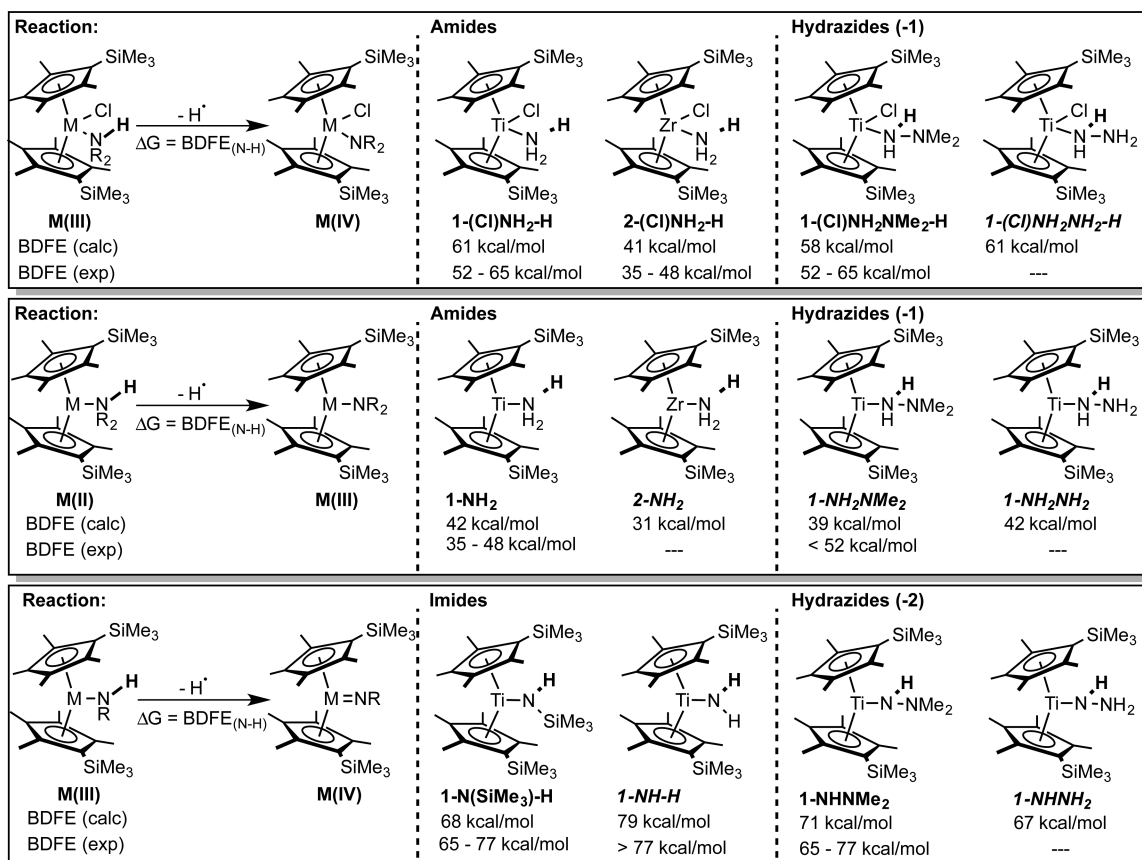


Figure 5. Summary of experimentally determined and calculated N–H bond dissociation free energies (BDFEs) in titanocene and zirconocene complexes. Key (Left to right): **Reaction:** Definition of the N–H BDFEs described in this work and associated redox state changes for metallocene complexes. **Amides:** N–H BDFEs for ammonia coordinated to either M(III) (top) or M(II) metal centers. Loss of H[•] results in the formation of the corresponding M(IV) or M(III) metal amide complex, respectively. **Hydrazides (-1):** N–H BDFEs for hydrazines coordinated to either Ti(III) (top) or Ti(II) metal centers. Loss of H[•] results in the formation of the corresponding Ti(IV) or Ti(III) metal hydrazide(-1) complex, respectively. **Imides/Hydrazides (-2):** N–H BDFEs for Ti(III) amides (top) and for Ti(III) hydrazides (bottom). Loss of H[•] results in the formation of the corresponding Ti(IV) imido (top) or Ti(IV) hydrazido (bottom) complex.

design of ammonia synthesis and oxidation catalysts, a combined experimental and computational study of N–H BDFEs in model titanocene and zirconocene complexes was conducted. The sterically demanding bis(cyclopentadienyl) ligand platform is ideally suited for this purpose as it enables preparation and isolation of metallocene complexes in the +3 and +4 oxidation and supports a variety of nitrogen-containing ligands, including rare “parent” derivatives where the substituents are exclusively hydrogen.⁴⁴

Our previous communication reported the N–H bond dissociation free energies of NH₃ coordinated to metallocenes with Ti(II), Ti(III), and Zr(III).²⁴ The N–H BDFE of 1-(Cl)NH₃ was calculated as 61 kcal/mol, consistent with the experimentally bracketed value of 52–65 kcal/mol. Notably substitution of the titanium(III) center with zirconium(III) plummets the N–H BDFE to 41 kcal/mol while reduction of Ti(III) to Ti(II) has a similar effect as the N–H BDFE in 1-NH₃ is 42 kcal/mol. The calculated values are in good agreement with experimental estimates of 35–48 kcal/mol. Analysis of the thermochemical data reveals that the difference in N–H BDFEs are driven principally by differences in redox potentials of the various metals. In cases where the redox couples have large and negative potentials such as Zr(IV)–Zr(III) and Ti(III)–Ti(II), weaker N–H BDFEs result.

With this foundation in hand, measurement of N–H BDFEs of other nitrogen-containing ligands relevant to a N₂ fixation scheme was conducted (Figure 5). Titanocene hydrazides were studied and exhibit similarities to the corresponding amide complexes. Addition of TEMPO[•] to a THF-*d*₈ solution containing 1-Cl in the presence of one equivalent of NH₂NMe₂ cleanly yielded 1-(Cl)NHNMe₂ and TEMPO-H, as judged by ¹H NMR spectroscopy and setting an upper limit of 65 kcal/mol for the N–H BDFE of the coordinated hydrazine.

Performing an analogous experiment with N₂H₄ also produced TEMPO-H along with free cyclopentadiene ligand and an unidentified high-symmetry organometallic complex. In the absence of N₂H₄, addition of TEMPO[•] to 1-Cl, produced no reaction. This observation suggests that the putative titanocene(III) intermediate, 1-(Cl)NH₂NH₂ is formed and undergoes H atom abstraction but the resulting parent titanocene(IV) chloro hydrazide, 1-(Cl)NHNH₂ is unstable. Because direct experimental evidence for 1-(Cl)NH₂NH₂ was not obtained, full molecule DFT calculations were conducted to gain insight into the N–H BDFE. A computed value of 61 kcal/mol was obtained, suggesting little perturbation upon dimethylation of the hydrazine. Similar measurements were attempted for the putative titanocene(II) hydrazine compound, 1-NH₂NMe₂.

Attempts to prepare **1-NH₂NMe₂** by formation of the N–H bond by addition of [Rh]-H to **1-NHNMe₂** produced no reaction. In the absence of an insurmountable kinetic barrier, this experiment establishes an upper limit on the BDFE of 52 kcal/mol, consistent with the DFT-computed value of 39 kcal/mol. A similar value of 42 kcal/mol was calculated for the corresponding parent hydrazide complex, **1-NH₂NH₂**, again highlighting little influence on nitrogen substitution on the N–H BDFE of the coordinated hydrazine. Perhaps unsurprisingly, ammonia and κ^1 -hydrazine ligands have indistinguishable N–H BDFEs when coordinated to titanocenes. This value may change upon a shift in hapticity to κ^2 ; however, attempts to optimize such structures resulted in reversion to κ^1 -hapticity.

Imido (Ti = NR) and hydrazido(2-) (Ti = NNH₂) complexes of titanocenes in the +3 and +2 oxidation states were also of interest. With this family of compounds, formation of an N–H bond is accompanied by reduction of a Ti = N π -bond. Addition of TEMPO-H to a THF-*d*₈ solution of **1=NSiMe₃** resulted in formation of TEMPO• and a new EPR-active titanocene(III) compound identified as (η^5 -C₅Me₄SiMe₃)₂Ti(NHSiMe₃) (**1-NHSiMe₃**). The titanocene imide, **1=NSiMe₃**, proved unreactive toward 2,4,6-^tBu₃PhO•, establishing an experimental N–H BDFE value in the range of 65–77 kcal/mol. The calculated N–H BDFE of 68 kcal/mol is in good agreement with the experimentally determined range. To experimentally determine the N–H BDFE in the parent imido compound (η^5 -C₅Me₄SiMe₃)₂Ti(NH) (**1=NH**), hydrogen atom abstraction from **1-NH₂** was explored using 2,4,6-^tBu₃PhO•. No reaction was observed between these two reagents over the course of hours at 23 °C. The lack of reactivity could be attributed to a high kinetic barrier, although this possibility seems unlikely given the facile H atom abstraction chemistry observed with 2,4,6-^tBu₃PhO• and other titanocenes. Thus, an experimental lower limit on the N–H BDFE is 77 kcal/mol. An upper limit on the N–H BDFE proved inaccessible as suitable noncoordinating reagents with known BDFEs in compatible solvents are unavailable. Nevertheless, the calculated N–H BDFE of **1-NH₂** (79 kcal/mol) is in good agreement with the experimental observations. Both experimental and calculated data indicate a ~10 kcal/mol difference in the BDFEs of **1-NHSiMe₃** and **1-NH₂**, highlighting the potential sensitivity of the thermodynamic parameters to silicon-containing substituents.

Titanocene(III) hydrazides(1-) (Ti-NHNR₂) were the final class of compounds examined. Hydrogen atom abstraction from **1-NHNMe₂** is expected to furnish the titanium hydrazide(2-) complex, (η^5 -C₅Me₄SiMe₃)₂Ti(NNMe₂) (**1=NNMe₂**). However, no reaction was observed upon treatment of **1-NHNMe₂** with TEMPO•, while treatment with 2,4,6-^tBu₃PhO• produced 2,4,6-^tBu₃PhO-H in 93% yield along with a mixture of unidentifiable titanium products. The instability of the putative complex, **1=NNMe₂**, is consistent with observations reported by Mountford and co-workers on the bonding of bis(cyclopentadienyl) titanium hydrazide (2-) complexes and their instability.^{45,46} The differential reactivity with TEMPO• and 2,4,6-^tBu₃PhO• supports an experimental BDFE of 65–77 kcal/mol, in good agreement with the calculated value of 71 kcal/mol. The hypothetical parent hydrazide complex, (η^5 -C₅Me₄SiMe₃)₂Ti(NHNH₂) (**1-NHNH₂**), was calculated to have an N–H BDFE of 67 kcal/mol. As was observed with **1-(Cl)NHNMe₂** and **1-(Cl)-NHNH₂**, the impact of methyl substituents on the N–H BDFEs is minimal and the experimentally determined BDFE

values for **1-(Cl)NHNMe₂** and **1-NHNMe₂** appear to be valid for the parent hydrazide(1-) analogues.

CONCLUSIONS

A family of bis(cyclopentadienyl) titanium and zirconium amide, hydrazide and imide complexes have been studied for N–H bond formation and ultimately catalytic amine or hydrazine synthesis by proton coupled electron transfer using H₂ as the stoichiometric H atom source. A combination of chemical bracketing studies coupled with DFT methods allowed determination of N–H bond dissociation free energies in 12 different complexes. In all cases examined, there is a significant lowering the N–H BDFE upon coordination to the transition metal. The impact of the metal identity, metal and nitrogen oxidation states on the N–H BDFE have been systematically determined where metals with relatively low redox potentials (e.g., Ti(III)–Ti(IV)) favor the highest values. Catalytic NH₃, NH₂SiMe₃ and NH₂NMe₂ synthesis has been demonstrated using [Rh–H] as the H₂ activation and H atom transfer catalyst. Although the chromium hydrides, [Cr–H] and [Cr]*-H have comparable M–H BDFEs to [Rh–H], the mismatched pK_a and reduction potentials associated with these reagents and the group 4 metallocene substrates resulted in low turnover due to catalyst deactivation. The outcomes of these studies demonstrate the value of N–H BDFEs in guiding the rational design and modification of both metal and ligand environments to generate complexes capable of catalytic ammonia synthesis, ideally from molecular N₂ and H₂.

ASSOCIATED CONTENT

Supporting Information

The Supporting Information is available free of charge on the ACS Publications website at DOI: 10.1021/jacs.6b08009.

Experimental procedures, full characterization data including NMR, EPR and infrared spectra, DFT output (PDF)

Crystallographic data (CIF)

AUTHOR INFORMATION

Corresponding Author

*pchirik@princeton.edu

Notes

The authors declare no competing financial interest.

ACKNOWLEDGMENTS

We thank the Director of the Office of Basic Energy Sciences, Chemical Sciences Division, U.S. Department of Energy (DE-FG-02-05ER15659) for financial support. We also thank Prof. Robert Knowles (Princeton) for helpful discussions.

REFERENCES

- (1) Tamaru, K. In *Catalytic Ammonia Synthesis*; Jennings, J. R., Ed.; Plenum: New York, 1991.
- (2) (a) *Nitrogen (fixed)—Ammonia*; U.S. Geological Survey, Mineral Commodity Summaries; U.S. Government Printing Office: Washington, D.C., 2016. (b) *Tracking Industrial Energy Efficiency and CO₂ Emissions*; International Energy Agency (IEA): Paris, 2007; pp 82–83.
- (3) Appl, M. *Ullmann's Encyclopedia of Industrial Chemistry* **2012**, 140–225.
- (4) (a) Peters, J. C.; Mehn, M. P. *Activation of Small Molecules: Organometallic and Bioinorganic Perspectives* **2006**, 81. (b) Chatt, J.; Richards, R. L. *J. Organomet. Chem.* **1982**, 239, 65.

- (5) (a) Chatt, J.; Dilworth, J. R.; Richards, R. L. *Chem. Rev.* **1978**, *78*, 589. (b) Hidai, M. *Coord. Chem. Rev.* **1999**, *185–186*, 99.
- (6) (a) Pickett, C. J.; Ryder, K. S.; Talarmin, J. J. *Chem. Soc., Dalton Trans.* **1986**, 1453. (b) Pickett, C. J.; Talarmin, J. *Nature* **1985**, *317*, 652.
- (7) (a) Shilov, A. E. *Russ. Chem. Bull.* **2003**, *52*, 2555. (b) Bazhenova, T. A.; Shilov, A. E. *Coord. Chem. Rev.* **1995**, *144*, 69–145.
- (8) (a) Kuriyama, S.; Arashiba, K.; Nakajima, K.; Tanaka, H.; Yoshizawa, K.; Nishibayashi, Y. *Chem. Sci.* **2015**, *6*, 3940. (b) Kuriyama, S.; Arashiba, K.; Nakajima, K.; Tanaka, H.; Kamaru, N.; Yoshizawa, K.; Nishibayashi, Y. *J. Am. Chem. Soc.* **2014**, *136*, 9719. (c) Arashiba, K.; Miyake, Y.; Nishibayashi, Y. *Nat. Chem.* **2011**, *3*, 120. (d) Yandulov, D. V.; Schrock, R. R. *Science* **2003**, *301*, 76.
- (9) (a) Ung, G.; Peters, J. C. *Angew. Chem., Int. Ed.* **2015**, *54*, 532. (b) Creutz, S. E.; Peters, J. C. *J. Am. Chem. Soc.* **2014**, *136*, 1105. (c) Anderson, J. S.; Rittle, J.; Peters, J. C. *Nature* **2013**, *501*, 84.
- (10) Del Castillo, T. J.; Thompson, N. B.; Suess, D. L. M.; Ung, G.; Peters, J. C. *Inorg. Chem.* **2015**, *54*, 9256.
- (11) Kuriyama, S.; Arashiba, K.; Nakajima, K.; Matsuo, Y.; Tanaka, H.; Ishii, K.; Yoshizawa, K.; Nishibayashi, Y. *Nat. Commun.* **2016**, *7*, 12181.
- (12) van der Ham, C. J. M.; Koper, M. T. M.; Hetterscheid, D. G. H. *Chem. Soc. Rev.* **2014**, *43*, 5183.
- (13) Macleod, K. C.; Holland, P. L. *Nat. Chem.* **2013**, *5*, 559.
- (14) Waidmann, C. R.; Miller, A. J. M.; Ng, C.-W. A.; Scheuermann, M. L.; Porter, T. R.; Tronic, T. A.; Mayer, J. M. *Energy Environ. Sci.* **2012**, *5*, 7771.
- (15) Connelly, N. G.; Geiger, W. E. *Chem. Rev.* **1996**, *96*, 877.
- (16) Fryzuk, M. D.; Johnson, S. A. *Coord. Chem. Rev.* **2000**, *200*, 379.
- (17) Fryzuk, M. D.; Love, J. B.; Rettig, S. J. *Science* **1997**, *275*, 1445.
- (18) (a) Pool, J. A.; Lobkovsky, E.; Chirik, P. J. *Nature* **2004**, *427*, 527. (b) Pool, J. A.; Bernskoetter, W. H.; Chirik, P. J. *J. Am. Chem. Soc.* **2004**, *126*, 14326.
- (19) (a) Chirik, P. J. *Dalton Trans.* **2007**, *1*, 16. (b) Semproni, S. P.; Chirik, P. J. *J. Am. Chem. Soc.* **2013**, *135*, 11373.
- (20) Sodium amalgam and silyl chlorides are an exception and compatible. Examples of catalytic N₂ silylation using this approach are well-documented. See for example: (a) Siedschlag, R. B.; Bernales, V.; Vogiatzis, K. D.; Planas, N.; Clouston, L. J.; Bill, E.; Gagliardi, L.; Lu, C. C. *J. Am. Chem. Soc.* **2015**, *137*, 4638. (b) Imayoshi, R.; Tanaka, H.; Matsuo, Y.; Yuki, M.; Nakajima, K.; Yoshizawa, K.; Nishibayashi, Y. *Chem. - Eur. J.* **2015**, *21*, 8905.
- (21) Warren, J. J.; Tronic, T. A.; Mayer, J. M. *Chem. Rev.* **2010**, *110*, 6961.
- (22) (a) Munisamy, T.; Schrock, R. R. *Dalton Trans.* **2012**, *41*, 130. (b) Nishibayashi, Y. *Inorg. Chem.* **2015**, *54*, 9234.
- (23) While experimental data for the N–H BDFEs of parent pyridinyl radicals is not available, the N–H BDFEs of Hantzsch ester derivatives have been determined to be 35–38 kcal/mol. See: Cheng, J.; Lu, Y.; Zhu, X.; Sun, Y.; Bi, F.; He, J. *J. Org. Chem.* **2000**, *65*, 3853.
- (24) Pappas, I.; Chirik, P. J. *J. Am. Chem. Soc.* **2015**, *137*, 3498.
- (25) (a) Hu, Y.; Norton, J. R. *J. Am. Chem. Soc.* **2014**, *136*, 5938. (b) Hu, Y.; Li, L.; Shaw, A. P.; Norton, J. R.; Sattler, W.; Rong, Y. *Organometallics* **2012**, *31*, 5058.
- (26) Related bond strengths have been calculated for (η^5 -C₅H₅)₂Ti(Cl)NR₂-H, but experimental thermochemical parameters were not determined. See: Paradis, M.; Campaña, A. G.; Jiménez, T.; Robles, R.; Oltra, J. E.; Buñuel, E.; Justicia, J.; Cárdenas, D. J.; Cuerva, J. M. *J. Am. Chem. Soc.* **2010**, *132*, 12748.
- (27) (a) Mankad, N. P.; Mu, P.; Peters, J. C. *J. Am. Chem. Soc.* **2010**, *132*, 4083. (b) Bowman, A. C.; Bart, S. C.; Heinemann, F. W.; Meyer, K.; Chirik, P. J. *Inorg. Chem.* **2009**, *48*, 5587. (c) Fantauzzi, S.; Gallo, E.; Caselli, A.; Ragaini, F.; Casati, N.; Macchi, P.; Cenini, S. *Chem. Commun.* **2009**, 3952. (d) King, E. R.; Betley, T. A. *Inorg. Chem.* **2009**, *48*, 2361. (e) Chomitz, W. A.; Arnold, J. *Chem. Commun.* **2008**, 3648. (f) Avenier, F.; Gouré, E.; Dubourdeaux, P.; Sénèque, O.; Oddou, J. L.; Pécaut, J.; Chardon-Noblat, S.; Deronzier, A.; Latour, J. M. *Angew. Chem., Int. Ed.* **2008**, *47*, 715. (g) Ni, C.; Fettinger, J. C.; Long, G. J.; Brynda, M.; Power, P. P. *Chem. Commun.* **2008**, 6045. (h) Badiel, Y. M.; Dinescu, A.; Dai, X.; Palomino, R. M.; Heinemann, F. W.; Cundari, T. R.; Warren, T. H. *Angew. Chem., Int. Ed.* **2008**, *47*, 9961. (i) Lucas, R. L.; Powell, D. R.; Borovik, A. S. *J. Am. Chem. Soc.* **2005**, *127*, 11596. (j) Shay, D. T.; Yap, G. P. A.; Zakharov, L. N.; Rheingold, A. L.; Theopold, K. H. *Angew. Chem., Int. Ed.* **2005**, *44*, 1508. (k) Kogut, E.; Wiencko, H. L.; Zhang, L.; Cordeau, D. E.; Warren, T. H. *J. Am. Chem. Soc.* **2005**, *127*, 11248. (l) Thyagarajan, S.; Shay, D. T.; Incarvito, C. D.; Rheingold, A. L.; Theopold, K. H. *J. Am. Chem. Soc.* **2003**, *125*, 4440. (m) Jensen, M. P.; Mehn, M. P.; Que, L. *Angew. Chem., Int. Ed.* **2003**, *42*, 4357. (n) Siewert, I. *Chem. - Eur. J.* **2015**, *21*, 15078.
- (28) (a) Milsman, C.; Semproni, S. P.; Chirik, P. J. *J. Am. Chem. Soc.* **2014**, *136*, 12099. (b) Wiese, S.; McAfee, J. L.; Pahls, D. R.; McMullin, C. L.; Cundari, T. R.; Warren, T. H. *J. Am. Chem. Soc.* **2012**, *134*, 10114. (c) Cowley, R. E.; Holland, P. L. *Inorg. Chem.* **2012**, *51*, 8352. (d) Iluc, V. M.; Miller, A. J. M.; Anderson, J. S.; Monreal, M. J.; Mehn, M. P.; Hillhouse, G. L. *J. Am. Chem. Soc.* **2011**, *133*, 13055. (e) Iluc, V. M.; Hillhouse, G. L. *J. Am. Chem. Soc.* **2010**, *132*, 15148. (f) Scepaniak, J. J.; Young, J. A.; Bontchev, R. P.; Smith, J. M. *Angew. Chem., Int. Ed.* **2009**, *48*, 3158. (g) Nieto, I.; Ding, F.; Bontchev, R. P.; Wang, H.; Smith, J. M. *J. Am. Chem. Soc.* **2008**, *130*, 2716. (h) Cowley, R. E.; Bontchev, R. P.; Sorrell, J.; Sarracino, O.; Feng, Y.; Wang, H.; Smith, J. M. *J. Am. Chem. Soc.* **2007**, *129*, 2424. For an example of separated PCET to diiron diazenides, hydrazides, and amides, see: (i) Li, Y. Y.; Wang, B.; Luo, Y.; Yang, D.; Tong, P.; Zhao, J.; Luo, L.; Zhou, Y.; Chen, S.; Cheng, F.; Qu, J. *Nat. Chem.* **2013**, *5*, 320.
- (29) Tilst, M. *Electron Transfer in Chemistry* **2001**, 766–713.
- (30) (a) Keppie, S. A.; Lappert, M. F. *J. Organomet. Chem.* **1969**, *19*, P5. (b) Fischer, E. O. *Inorg. Synth.* **1963**, *VII*, 136. (c) King, R. B.; Stone, F. G. A. *Inorg. Synth.* **1963**, *VII*, 99.
- (31) (a) Hartung, J.; Norton, J. R. *Catalysis Without Precious Metals* **2010**, 1–24. (b) Tilst, M. *J. Am. Chem. Soc.* **1992**, *114*, 2740. (c) Parker, V. D.; Handoo, K. L.; Roness, F.; Tilst, M. *J. Am. Chem. Soc.* **1991**, *113*, 7493. (d) Tilst, M.; Parker, V. D. *J. Am. Chem. Soc.* **1989**, *111*, 6711. (e) Jordan, R. F.; Norton, J. R. *J. Am. Chem. Soc.* **1982**, *104*, 1255.
- (32) (a) Estes, D. P.; Norton, J. R.; Jockusch, S.; Sattler, W. J. *Am. Chem. Soc.* **2012**, *134*, 15512. (b) Smith, D. M.; Pulling, M. E.; Norton, J. R. *J. Am. Chem. Soc.* **2007**, *129*, 770. (c) Tang, L.; Papish, E. T.; Abramo, G. P.; Norton, J. R.; Baik, M.-H.; Friesner, R. A.; Rappé, A. J. *Am. Chem. Soc.* **2003**, *125*, 10093.
- (33) (a) Bullock, R. M.; Samsel, E. G. *J. Am. Chem. Soc.* **1990**, *112*, 6886. (b) Miyake, A.; Kondo, H. *Angew. Chem., Int. Ed. Engl.* **1968**, *7*, 631.
- (34) (a) Baird, M. C.; Jaeger, T. J. *Organometallics* **1988**, *7*, 2074. (b) Leoni, O.; Landi, A.; Pasquali, M.; A. E. S. S.; Leoni, O.; Landi, A.; Pasquali, M. *J. Organomet. Chem.* **1987**, *321*, 365.
- (35) Vol'pin, M. E.; Shur, V. B. *Nature* **1996**, *209*, 1236.
- (36) (a) Schwarz, A. D.; Onn, C. S.; Mountford, P. *Angew. Chem., Int. Ed.* **2012**, *51*, 12298. (b) Janssen, T.; Severin, R.; Diekmann, M.; Friedemann, M.; Haase, D.; Saak, W.; Doye, S.; Beckhaus, R. *Organometallics* **2010**, *29*, 1806.
- (37) (a) Pietryga, J. M.; Jones, J. N.; MacDonald, C. L. B.; Moore, J. A.; Cowley, A. H. *Polyhedron* **2006**, *25*, 259. (b) Ubn, D. U.; Eselsberg, O.; Leigh, G. J.; Walker, D. G. *J. Organomet. Chem.* **1987**, *323*, C29. (c) Dilworth, J. R.; Latham, I. A.; Leigh, G. J.; Huttner, G.; Jibril, I. J. *Chem. Soc., Chem. Commun.* **1983**, 1368.
- (38) (a) Hanna, T. E.; Lobkovsky, E.; Chirik, P. J. *Eur. J. Inorg. Chem.* **2007**, *2007*, 2677. (b) Hanna, T. E.; Keresztes, I.; Lobkovsky, E.; Bernskoetter, W. H.; Chirik, P. J. *Organometallics* **2004**, *23*, 3448.
- (39) Marbach, P.; Chaney, L. *Clin. Chem.* **1961**, *130*.
- (40) For a comprehensive table of pK_a values in THF, see: Rodima, T.; Kaljurand, I.; Pihl, A.; Mäemets, V.; Leito, I.; Koppel, I. a. *J. Org. Chem.* **2002**, *67*, 1873.
- (41) Notably, our calculation of the [Cr]*-H BDFE in THF using a pK_a value of 10.1, E_{red} value of –0.83V, and correction constant in THF of 66 kcal/mol yields 60.7 kcal/mol, in good agreement with the literature value of 58 kcal/mol in MeCN. There may be error in this value due to ion pairing effects and uncertainty in the correction

constant for THF. Concerning the correction constant in THF, see:

(a) Tilset, M. *Electron Transfer in Chemistry* **2001**, 766–713.

(b) Cappellani, E. P.; Drouin, S. D.; Jia, G.; Maltby, P. A.; Morris, R. H.; Schweitzer, C. T. *J. Am. Chem. Soc.* **1994**, *116*, 3375.

(42) In ref 21 we reported the peak cathodic potentials due to the observed electrochemical irreversibility. A comparison of the peak cathodic potentials amongst the structurally similar metallocene complexes was sufficient to establish trends. For the present purposes, we have estimated the equilibrium reduction potentials of $[1\text{-NH}_3]^+$, $[1\text{-(Cl)NH}_3]^+$, and $[2\text{-(Cl)NH}_3]^+$ as -2.0 , -1.1 , and -2.0 V, respectively, using the known pK_a values, calculated BDFEs, and correction constant in THF of 66.

(43) Hamilton, D. M.; Willis, W. S.; Stucky, G. D. *J. Am. Chem. Soc.* **1981**, *103*, 4255.

(44) For examples relevant to N_2 fixation, see reference 24 and (a) Anderson, J. S.; Moret, M. E.; Peters, J. C. *J. Am. Chem. Soc.* **2013**, *135*, 534. (b) Yandulov, D. V.; Schrock, R. R. *Inorg. Chem.* **2005**, *44*, 1103.

(45) (a) Tiong, P. J.; Groom, L. R.; Clot, E.; Mountford, P. *Chem. - Eur. J.* **2013**, *19*, 4198. (b) Selby, J. D.; Feliz, M.; Schwarz, A. D.; Clot, E.; Mountford, P. *Organometallics* **2011**, *30*, 2295.

(46) For examples of stable titanium hydrazide (-2) complexes, see also: (a) Tiong, P. J.; Nova, A.; Schwarz, A. D.; Selby, J. D.; Clot, E.; Mountford, P. *Dalton Trans.* **2012**, *41*, 2277. (b) Selby, J. D.; Manley, C. D.; Feliz, M.; Schwarz, A. D.; Mountford, P. *Chem. Commun.* **2007**, 4937. (c) Parsons, T. B.; Hazari, N.; Cowley, A. R.; Green, J. C.; Mountford, P. *Inorg. Chem.* **2005**, *44*, 8442.